Chapter 10

Comparison Between GPS Sea Surface Heights, MSS Models and Satellite Altimetry Data in the Aegean Sea. Implications for Local Geoid Improvement

I. Mintourakis and D. Delikaraoglou

Abstract We have conducted various experiments of sea surface height (SSH) measurements in Greece's Aegean Sea using on-board kinematic GPS recordings and the KMSS04 satellite altimetry-derived mean sea surface for comparison. This region is of particular interest because of strong crustal movements due to intense tectonic activity that create significant local geoid variations. In this paper, we report on the results of separate SSH surveys that were conducted in three test areas in the Aegean Sea. Ship borne GPS data were collected together with GPS data simultaneously collected at nearby mainland reference stations. These high rate data were processed in kinematic mode using scientific GPS software and related to SSH observations, thus allowing us to obtain maps of the instantaneous sea surface, which was estimated with a precision at the level of a few centimeters. Tidal recordings from nearby tidal stations provided us with the required tidal corrections for the reduction of the GPS-derived SSHs to mean sea level (MSL). Following a filtering process, a cross over adjustment and gridding of the pointwise SSH observations in each test area, local maps of the mean sea surface (MSS) were obtained, which can be compared with the available KMSS04 global solution for the MSS. To examine further the MSS-related results that we observed in these experiments, we compared both the GPS-derived and the KMSS04-related MSS with JASON-1 radar altimetry and ICEsat laser altimetry data over the same areas. We show that the SSHs derived from the GPS ship surveys, when carefully analyzed and applying suitable filtering techniques and necessary corrections for the Dynamic Ocean Topography (DOT) can provide enhanced shorter wavelength components of the local geoid. This is illustrated with additional comparisons with the EGM96 and EGM08 global geoid models, in order to reveal any significant differences, mainly in the short wavelength domain, when compared to the aforementioned local geoid models computed from purely GPS-derived SSH data.

10.1 Introduction

The use of GPS receivers for collecting Sea Surface Height (SSH) data has been implemented mostly with the use of GPS equipped buoys for satellite radar altimetry calibrations (Born et al., 1994), while ship borne GPS SSH campaigns are quite rare, mainly because of the high costs associated with such sea trials.

The current project was motivated initially by the lack of regular SSH campaigns in Greece, so that when the opportunity presented itself it was decided to collect SSH data with a GPS receiver installed on the Hellenic Navy's Hydrographic Service vessel R/V NAUTILUS during some of its regular hydrographic surveys. Thus we have collected SSH data during three hydrographic cruises from May 2006 to September 2007, in the areas shown in Fig. 10.1. The GPS receivers used in the project were the Daussault Sercel SCORPIO 6002 (land survey) and AQUARIUS 5002 (marine survey) types. Both receivers are 12-channel, dual frequency instruments using DSNP NAP geodetic

I. Mintourakis (✉)
Department of Surveying Engineering, National Technical University of Athens, Zografos 15780, Greece
e-mail: mintioan@survey.ntua.gr

S.P. Mertikas (ed.), *Gravity, Geoid and Earth Observation*, International Association of Geodesy Symposia 135,
DOI 10.1007/978-3-642-10634-7_10,

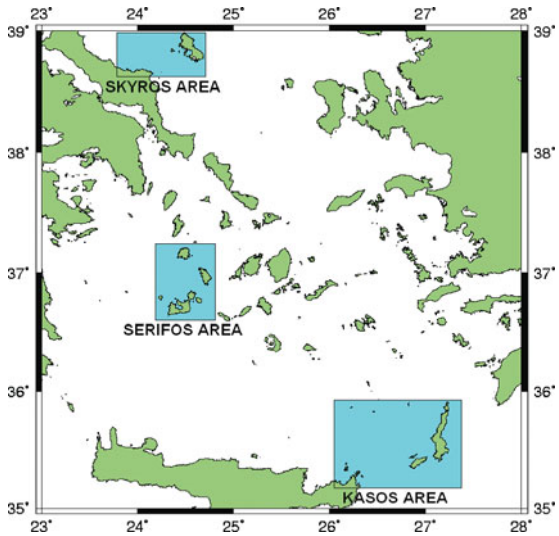

Fig. 10.1 Location of test areas

antennas and allowing code and phase observations on L1 and L2. Both systems are capable of LRK (long range kinematic) techniques and feature UHF coverage of up to 40 km, initialization time of a few seconds and 1–2 cm accuracy at 1-s sampling rate. The receivers operated at 1 Hz recording rate, thus offering a wealth of instantaneous SSH measurements with extremely high spatial resolution in the areas of operation.

Initial processing included the necessary reductions of the GPS SSH data to Mean Sea Level (MSL) using nearby tidal stations and a crossover adjustment. Subsequently, we made comparisons of the GPS-derived MSS results with the global mean sea surface model KMSS04 (Knudsen et al., 2005), which is the result of a combine solution of 9-year (1993–2001) repeated and averaged over time altimetry observations from multiple altimetry satellites (TOPEX/Poseidon, ERS-1 and -2, GEOSAT, and GFO).

From a preliminary inspection of the observed mean differences between the GPS-derived MSL and the KMSS04 MSS, ($MSL_{GPS} - MSS_{KMSS04}$), we concluded that there were some small biases present in the data, which ranged from –9 cm in the data collected in the region between Serifos, Sifnos, and Kimolos islands (hereby designated as *Serifos area*), to 23 cm in the region between Crete, Kasos and Karpathos islands (designated as *Kasos area*) and only 1 cm in the region between Skyros and Evia islands (designated as *Skyros area*). We first suspected that a likely influence for these biases had to do with the various tide systems used, i.e. the fact that the KMS04 MSS is given in the Mean tide system (MTS) whereas in the GPS processing (because of its inherently geometric positioning nature) the no tide system (NTS) is used. Typically, in marginal seas, this can give a latitudinal offset in the range of 10–20 cm. However, there is no evidence for this occurring in our test areas, considering also that the tides are particularly weak in these parts of the Aegean Sea. Instead, we feel that a large part of these biases can be attributed to unaccounted vessel vertical motion effects, which in our case were not possible to compensate for because of the lack of an onboard inertial navigation system (INS) and/or a heave-measuring sensor, which otherwise would help to correct for some of these effects during each cruise. In particular, the higher mean difference noted for the data collected in the Kasos area can be attributed to a lower precision (up to a few centimetres) of the antenna height measurement with respect to the vessels static waterline, and the changes in the vessel's payload during the specific survey trip, as well as the effect of the vessel's speed on the determination of the waterline (i.e. the influence of dynamic draft).

In order to alleviate these recognized weaknesses in our measuring process, it was decided to use the KMSS04 model as a reference surface for the data of each cruise. Therefore all GPS-derived SSHs were "leveled" to KMS04 by removing the observed bias for each of the three major cruises, thus reducing our data from the NTS to the MTS system. Subsequently, the strategy that was followed was to apply first an along-track time domain filter, followed by a reduction of the instantaneous SSH measurements to MSL with the use of mean monthly sea level anomalies from nearby tide gauges, and lastly, by performing a cross over adjustment of all kinematic GPS trajectories in order to minimize the sea height differences across the entire area of each experiment.

For each of these processing steps, we present in the sequel descriptive statistics of the corresponding comparisons with the KMSS04 mean sea surface in order to illustrate the amount of improvement in the results that was achieved at each step of this process. Most of our computations were done using the Generic Mapping Tools suite (GMT).

The major objective in this effort is to demonstrate the potential of shipborne GPS SSH measurements to produce accurate MSS maps inherently containing information about the short wavelength variations of

the local geoid in the areas of our tests. Hence, in order to validate further the results of these experiments, we made additional comparisons with the EGM96 (Lemoine et al., 1998) and EGM08 (Pavlis et al., 2008) global geoid models and the so-called Self-Consistent Synthetic Geoid regional model over Greece (SCSGGr) that has been produced and is distributed on a $5' \times 5'$ grid by the IAG Special Study Group SSG3.177 (2002).

10.2 Processing of GPS Derived SSH Data

10.2.1 Along Track Filtering

Our instantaneous GPS SSH measurements were contaminated (a) by high frequency noise mostly due to roll and pitch movements of the vessel while travelling in variable sea wave conditions, and (b) by the occasional difficulties to resolve the integer phase ambiguities of the kinematic GPS solutions.

In order to smooth the instantaneous SSH data we have applied different along track filters in the time domain. Initially we tried various options, such as, for example, the boxcar-, the cosine arch- and the Gaussian-type convolution filters, each with resolutions varying from 200 s to 1,200 s, and concluded that there were insignificant differences among these types of filters for the same resolutions. Therefore, it was decided to apply throughout a time domain Gaussian filter of 600 s resolution, which for an average vessel speed of 4 m/s corresponds to 2.4 km full wavelength (or 1.2 km spatial resolution). In addition, we applied a rejection criterion for any along-track data gaps exceeding 60 s duration.

The application of Gaussian filtering on the collected GPS SSH data, as compared with the KMSS04 model in a total of 10,20,711 points, resulted in a significant improvement. As shown in Table 10.1, this improvement is evident from the pre- and after-filtering minimum and maximum differences and their range by almost 50%, as well as the noticeable improvement in the corresponding standard deviations.

10.2.2 Reduction of GPS Sea Surface Heights to MSL

In order to reduce the filtered GPS sea surface heights to MSL we have used monthly tidal records from nearby tide gauge stations. This step required to bring each of the tidal datasets to an unbiased estimate of MSL at a common epoch, to express them all in a common datum, and to interpolate them into a continuous mean sea surface. These steps allowed us to produce a grid of sea level anomalies (SLA) using a tension surface algorithm. Although the SLAs are quite small in the Aegean Sea (ranging only to a few centimetres) special consideration was paid on the choice of the location of appropriate tide gauges that were used for this purpose. Subsequently, the reduction of each SSH measurement to MSL required an interpolation from the generated SLA grid to the location of each measurement point.

Diurnal sea level variations, which can also account for a few centimetres (i.e. not more than 10 cm, for most of the cases) were left to be treated through the subsequent cross over adjustment process. As shown in Table 10.2, the reduction to MSL, using monthly tidal records, brought the mean difference of the GPS-derived MSL and KMSS04 down to the millimetre level, also suggesting that the use of monthly tidal records was adequate for our purpose and there was little to be gained by using, for example, hourly or even daily SLA values.

Table 10.1 Statistics of the discrepancies between GPS-derived SSH and KMSS04 MSS as a result of along-track filtering

Mean (m)	Standard deviation (m)	Min (m)	Max (m)	Range (m)
Before along track filtering				
0.020	0.124	−1.482	1.485	2.967
After along track filtering				
0.020	0.112	−0.580	0.950	1.530

Table 10.2 Statistics of the discrepancies between GPS-derived MSL and KMSS04 MSS following SSH to MSL reductions

Mean (m)	Standard deviation (m)	Min (m)	Max (m)	Range (m)
Before reduction to MSL				
0.020	0.112	−0.580	0.950	1.530
After reduction to MSL				
−0.001	0.113	−0.633	0.928	1.561

10.2.3 Cross Over Adjustment

Cross over errors at the intersections of the vessel's GPS trajectories, in our case, can be attributed mostly to the difference, during the various legs of a cruise, in the vessel's draft caused by the change of its tonnage due to fuel usage and water consumption or any significant changes in the weight of its carried equipment (e.g. boat loading variances during the course of a survey). Considering the length of each cruise, in our case, it was considered adequate to implement a least squares cross over adjustment model consisting of a constant shift and a time drift.

For the implementation of the cross over adjustment methodology we divided our data to daily cruises and used the "x_over" module of GMT to perform the necessary computations (Wessel, 1989). Based on a total of 1,008 crossover points in all three test areas, the adjustment results showed a mean of the cross over differences of −0.011 m and a standard deviation of 0.111 m before adjustment, and after the adjustment these respective values fell to a mean of −0.001 m and a standard deviation of 0.059 m. The latter value should be interpreted as the internal accuracy of our dataset after the cross over adjustment. A slight improvement was noted in the statistics of the cross over adjustment-corrected GPS MSL dataset as compared to KMSS04. The improvement of the GPS-derived MSL dataset after the cross over adjustment becomes more evident in the first two test areas (i.e. the Serifos area and the Kasos area respectively) while there is a slight deterioration in the statistics for the Skyros area, as shown in Table 10.3, which needs to be examined further. The later could be attributed to the combination of very steep bathymetry near the shore and the fact that the major part of the comparison is held in a narrow zone very close to the coast where the KMSS04 satellite altimetry derived MSS possibly have a reduced quality.

Table 10.3 Statistics, per region of experiments, of the discrepancies between GPS-derived MSL and KMSS04 MSS following the cross over adjustment

Mean (m)	Standard deviation (m)	Min (m)	Max (m)	Range (m)
Serifos area before COA (4,66,705 SSH points)				
0.011	0.096	−0.280	0.298	0.578
Serifos area after COA				
0.003	0.065	−0.235	0.218	0.453
Kasos area before COA (3,21,498 SSH points)				
−0.025	0.129	−0.633	0.304	0.937
Kasos area after COA				
−0.006	0.112	−0.604	0.296	0.900
Skyros area before COA (2,19,156 SSH points)				
−0.009	0.115	−0.374	0.345	0.720
Skyros area after COA				
0.010	0.134	−0.383	0.437	0.821

10.2.4 Gridding and Smoothing of Datasets

As a final processing step, in order to produce the required MSS maps it was necessary to implement a gridding process on the cross over-adjusted GPS MSL data points, accompanied by a smoothing of the generated grid for each test area. For this purpose we used an adjustable tension continuous curvature surface algorithm, together with a Gaussian filter in the spatial domain with a 4 arcmin full wavelength, for the purpose of smoothing the final grids. The final MSS maps were computed with a resolution of 15 arcsec (i.e. grid spacing 450 m). These were then compared to KMSS04 for each region and the results are shown in Table 10.4. Due to the space limitations in this paper, we only show in Figs. 10.2 and 10.3 the respective maps for the Serifos area.

10.3 Comparisons with JASON-1 and ICESat Altimetry Data

In two of our test areas, we were able to make a further comparison of the final MSS, in each case, with the altimetry observations of the JASON-1 subtrack number 094 (cycles 70 through 205), which was crossing both areas. This subtrack descends from the Chalkidiki peninsula passing west of the island of

Table 10.4 Statistics of the discrepancies between the final GPS-derived MSS (gridded GPS-derived MSL) and KMSS04 MSS

Mean (m)	Standard deviation (m)	Min (m)	Max (m)	Range (m)
Serifos area MSS				
0.012	0.063	−0.141	0.187	0.328
Kasos area MSS				
−0.038	0.086	−0.286	0.166	0.451
Skyros area MSS				
0.043	0.111	−0.235	0.400	0.635

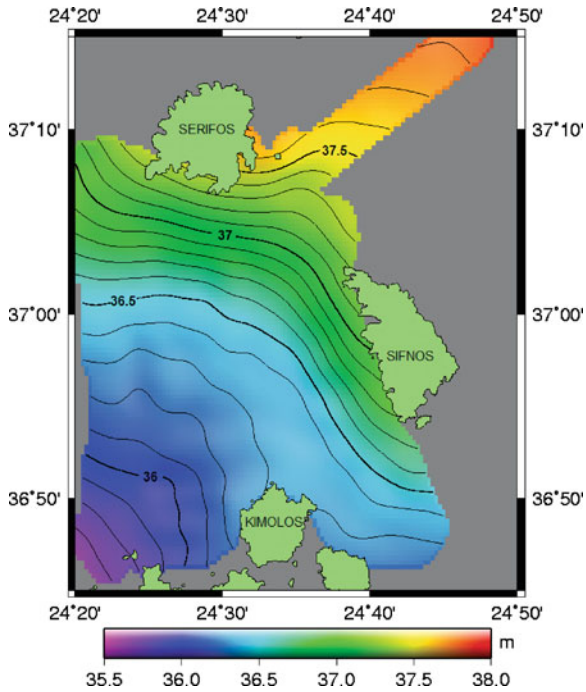

Fig. 10.2 Final GPS-derived MSS computed for the Serifos area

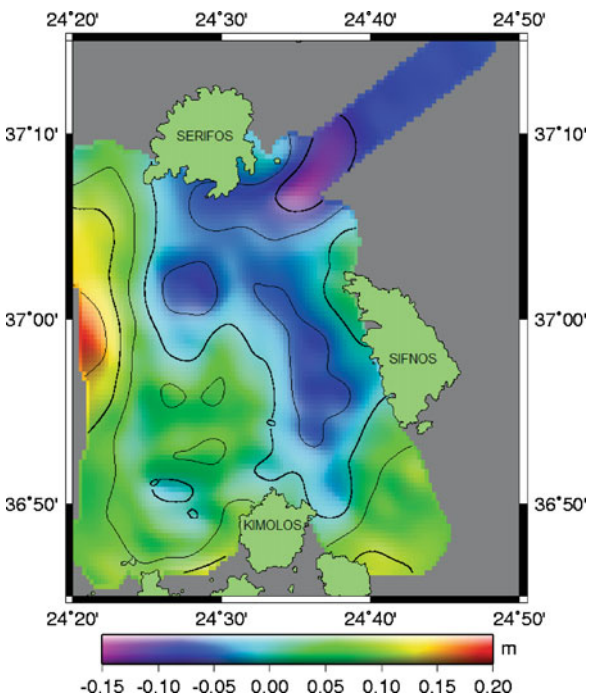

Fig. 10.3 Difference between the final MSS and KMSS04 for the Serifos area

Skyros and through the Kasos-Creta straight. For this purpose we use the data from the AVISO Geophysical Data Records (GDRs) and applied all the range corrections provided, namely: for the dry troposphere (model ECMWF) and the radiometer wet tropospheric correction on Ku-band, together with ionospheric and sea state bias corrections, as well as inverse barometer and tidal (FES99 model) corrections.

Similar comparisons were possible with the laser altimetry observations, covering all three areas of interest, from several subtracks of the Ice, Cloud, and land Elevation Satellite (ICESat) for the satellite's operational periods from 2003 till 2007. For these comparisons, we use pre-processed ICESat altimetry observations, without any additional reductions (e.g. stacking or cross over adjustments). In Tables 10.5 and 10.6 we present the statistics of the differences obtained between the altimetry observations from each of these satellites and the KMSS04 model. It should be noted that in both of these tables, the comparisons shown between the GPS-derived MSS smoothed grids and the KMSS04 are made on the locations of each altimetry footprint, and not for the entire grid as it was done for the similar comparisons shown in Table 10.4.

Table 10.5 Statistics of the discrepancies of pair combinations between the JASON-1 footprints, the GPS-derived MSS smoothed grids and the KMSS04

Delta	Mean (m)	Standard deviation (m)
JASON-*Kasos area* MSS	0.248	0.151
JASON-KMSS04	0.196	0.140
Kasos area MSS-KMSS04	−0.052	0.042
JASON-*Skyros area* MSS	0.142	0.137
JASON-KMSS04	0.191	0.138
Skyros area MSS-KMSS04	0.048	0.048

Table 10.6 Statistics of the discrepancies of pair combinations between the ICESat footprints, the GPS-derived MSS smoothed grids and KMSS04

Delta	Mean (m)	Standard deviation (m)
ICE-*Serifos area* MSS	−0.135	0.208
ICE-KMSS04	−0.121	0.213
Serifos area MSS-KMSS04	0.014	0.056
ICE-*Kasos area* MSS	0.028	0.251
ICE-KMSS04	0.006	0.254
Kasos area MSS-KMSS04	−0.022	0.066
ICE-*Skyros area* MSS	−0.164	0.218
ICE-KMSS04	−0.092	0.188
Skyros area MSS-KMSS04	0.072	0.124

From the results shown in Table 10.5, it is clearly seen that there are small differences, i.e. at the 5 cm level for the corresponding mean differences, and at the cm level for the Standard Deviations, for the comparisons of the JASON footprints and both the regional MSSs and KMSS04. It is also noticeable that the comparisons between KMSS04 and JASON-1 SSHs give almost identical results for both test areas.

Similarly, it is evident from Table 10.6, that there are no significant differences (i.e. at the 1–2 cm level for the corresponding mean differences, and at the sub-cm level for the Standard Deviations) in the comparisons between the ICEsat footprints data and both the regional MSSs and KMSS04 for the test areas of Serifos and Kasos islands. The corresponding results seem to be slightly worse for the area of Skyros Island (i.e. at more that 7 cm in the mean differences, and 3 cm in the Standard Deviations).

10.4 Comparisons with Global and Local Geoid Models

The MSS models generated from the GPS data contain both the geoid and the Dynamic Ocean Topography (DOT) signals. Therefore, in order to make meaningful comparisons with various geoid models it is necessary to remove the DOT signal from the estimated MSS. To do so, we used the DNSC08 MDT global model (Andersen and Knudsen, 2008) and made further comparisons of the resulting local marine geoid models with the EGM96 and EGM08 geopotential models and the existing SCSGGr geoid model. The results of these comparisons are shown in Table 10.7

To illustrate the differences of the new local geoid models versus EGM2008, the results for the Serifos area are depicted in Fig. 10.4, together with topography-bathymetry contours from the SRTM30 model. Although the SRTM30 is not accurate enough or even with the appropriate resolution, one can see the very close agreement between the major local topography-bathymetry variations described by the SRTM30 model and the corresponding variations described by the local geoid model in this area. It is clear that these local variations are strongly related to topography signal and that the new local geoid models that were derived purely from marine GPS measurements, are capable to depict short topography variations and have the potential to provide enhanced shorter wavelength components of the geoid.

Table 10.7 Statistics of the differences between the GPS-derived local marine geoid(s) and EGM96/08, SCSGGr geoid models

	Mean (m)	Standard deviation (m)
Serifos area geoid EGM08	0.267	0.087
Serifos area geoid EGM96	−0.133	0.158
Serifos area geoid SCSGGr	−0.654	0.072
Kasos area geoid EGM08	−0.240	0.124
Kasos area EGM96	−0.514	0.306
Kasos area SCSGGr	−1.341	0.119
Skyros area geoid EGM08	0.191	0.232
Skyros area geoid EGM96	−0.248	0.266
Skyros area geoid SCSGGr	−0.638	0.198

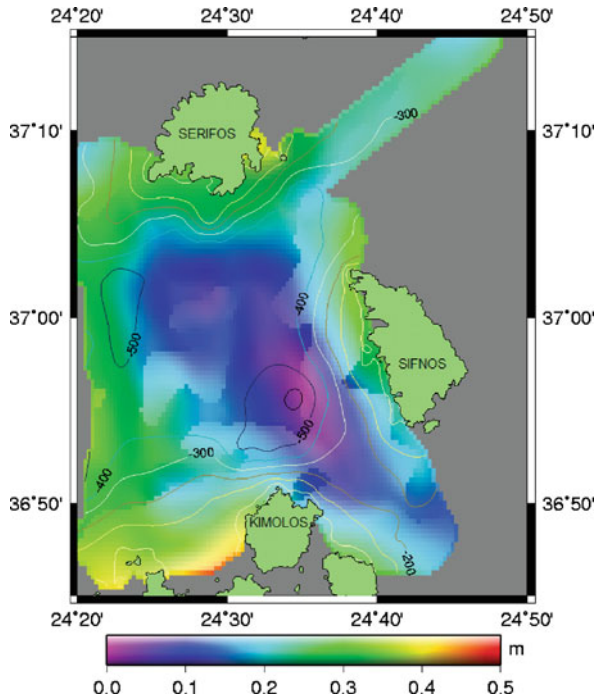

Fig. 10.4 Undulation differences between the local geoid model in the area of Serifos and the EGM2008 geoid. Topography-bathymetry contours are plotted at 200 m interval

10.5 Conclusions

Although these first results seem encouraging there are still a number of improvements possible in the methodology just outlined. Obviously, better results may be possible by using additional shipborne equipment in aid of the GPS receiver, such as an INS unit and a heave-draught correction sensor, which

could aid the compensation of many adverse effects of the vessel's motion, speed variations and sea wave conditions.

As this is a preliminary study, in our follow up investigations we plan to pursue a number of refinements, such as accounting for other contributions to sea level variations (e.g. seasonal heating and expansion of the sea surface), as well as further refinements in the GPS derived SSH data processing techniques (e.g. using daily or even hourly tidal corrections instead of monthly values) and experimenting with different crossover adjustment strategies (e.g. steady course vs. daily duration cruise legs).

References

Andersen, O.P. and P. Knudsen (2008). The DNSC08MDT mean dynamic topography. European Geosciences Union General Assembly, Vienna, Austria, April13–18.

Born, G.H., M.E. Parke, P. Axelrad, K.L. Gold, J. Johnson, K.W. Key, D.G. Kubitschek, and E.J. Christensen (1994). Calibration of the TOPEX altimeter using a GPS buoy. *J. Geophys. Res.*, *99*(C12), 24517–24526.

IAG Special Study Group SSG3.177 (2002). Synthetic modelling of the Earth's gravity field. Availabe at http://www.cage.curtin.edu.au/∼will/ssgres.html (Last accessed on June 18, 2008).

Knudsen, P., A.L. Vest, and O. Andersen (2005). Evaluating mean dynamic topography models within the GOCINA project. ESA SP–572, April.

Lemoine, F.G., S.C. Kenyon, J.K. Factor, R.G. Trimmer, N.K. Pavlis, D.S. Chinn, C.M. Cox, S.M. Klosko, S.B. Luthcke, M.H. Torrence, Y.M. Wang, R.G. Williamson, E.C. Pavlis, R.H. Rapp, and T.R. Olson (1998). The development of the joint NASA GSFC and the National Imagery and Mapping Agency (NIMA) geopotential model EGM96. *NASA Tech. Pub. 1998-206861*, Goddard Space Flight Center, Greenbelt, MD.

Pavlis, N.K., S.A. Holmes, S.C. Kenyon, and J.K. Factor (2008). An earth gravitational model to degree 2160: EGM2008. Presentation given at the 2008 European Geosciences Union General Assembly, Vienna, Austria, April1 3–18.

Wessel, P. (1989). XOVER: A cross-over error detector for track data. *Comput. Geosci.*, 15, 333–346.